Nakanishi, M., & Tsuobi, M. (1978a) *J. Am. Chem. Soc. 100*, 1273–1275.
Nakanishi, M., & Tsuboi, M. (1978b) *Chem. Phys. Lett. 57*, 262–264.
Nakanishi, M., & Tsuboi, M. (1979) *Bull. Chem. Soc. Jpn. 52*, 1337–1339.
Nakanishi, M., Nakamura, H., Hirakawa, A. Y., Tsuboi, M., Nagamura, T., & Saijo, Y. (1978) *J. Am. Chem. Soc. 100*, 272–276.
Sato, S., & Tamiya, N. (1970) *J. Biochem. (Tokyo) 68*, 867–872.
Sato, S., & Tamiya, N. (1971) *Biochem. J. 122*, 453–461.
Seto, A., Sato, S., & Tamiya, N. (1970) *Biochim. Biophys. Acta 214*, 483–489.
Shinitzky, M., & Fridkin, M. (1976) *Biochim. Biophys. Acta 434*, 137–143.
Stryer, L. (1966) *J. Am. Chem. Soc. 88*, 5708–5712.
Tamiya, N., & Arai, H. (1966) *Biochem. J. 99*, 624–630.
Tamiya, N., & Abe, H. (1972) *Biochem. J. 130*, 547–555.
Tsernoglou, D., & Petsko, G. A. (1977) *Proc. Natl. Acad. Sci. U.S.A. 74*, 971–974.

Nuclear Magnetic Resonance Determination of Metal–Proton Distances in the EF Site of Carp Parvalbumin Using the Susceptibility Contribution to the Line Broadening of Lanthanide-Shifted Resonances†

Lana Lee and Brian D. Sykes*

ABSTRACT: The substitution of the paramagnetic lanthanide ion ytterbium for the calcium ion in the EF calcium binding site of carp parvalbumin results in a series of ^{1}H NMR resonances which are shifted well outside of the envelope of the ^{1}H NMR spectrum of the diamagnetic form of the protein. The line broadening of these shifted resonances has been measured as a function of ^{1}H NMR frequency between 200 and 400 MHz, and the spin–lattice relaxation rates have been measured at 270 MHz. The analysis of the relaxation rates based upon the theories of Vega & Fiat [Vega, A. J., & Fiat, D. (1976) *Mol. Phys. 31*, 347–355] and Guêron [Guêron, M. (1975) *J. Magn. Reson. 19*, 58–66] indicates that a major contribution to the line widths comes from the novel susceptibility relaxation mechanism and that the metal to proton distances can be directly calculated from this contribution.

Calcium binding proteins play an important role in the regulation of many biochemical processes (Kretsinger, 1976; Rasmussen et al., 1972). Among the most studied of these proteins are the skeletal and cardiac troponins (Potter et al., 1977) and the myosin light chains (Weeds et al., 1977) which are involved in the regulation of muscle contraction and calmodulin which is involved in the regulation of bovine brain phosphodiesterase (Lin et al., 1974), brain adenylate cyclase (Westcott et al., 1979), chicken gizzard myosin light-chain kinase (Dabrowska et al., 1978), rabbit skeletal myosin light-chain kinase (Yagi et al., 1978), and a number of other enzymes [for a recent review, see Cheung (1980)]. The elucidation of the X-ray structure of the calcium binding protein parvalbumin from carp revealed that its two calcium binding sites are each completely formed from a contiguous polypeptide sequence folded into the homologous "CD and EF hands" (Kretsinger & Nockolds, 1973). Each homologous calcium binding domain contains in turn a helix, a loop around the metal ion, and a second helix. The loop around the metal ion contains regularly spaced liganding carboxyl, carbonyl, or hydroxyl ligands. Homologous sequences to parvalbumin (Kretsinger, 1976) can be found in rabbit skeletal troponin C and myosin alkali light chains (Collins, 1974; Weeds & McLachlan, 1974), DTNB light chains (Collins, 1976), bovine calmodulin (Vanaman et al., 1977; Stevens et al., 1976), rat testis calmodulin (Dedman et al., 1978), bovine intestinal calcium binding protein (Fullmer & Wasserman, 1977), porcine intestinal calcium binding protein (Hofmann et al., 1979), and other calcium binding proteins. The number of times in a given protein the sequence repeats and the substitutions therein can be correlated with the number of metals bound to the protein and their binding strengths, respectively. These findings have lead to the proposal that homologous structures, at least at the level of the calcium binding sites, exist for all these proteins.

In a separate paper (Lee & Sykes, 1980b) we have described the strategy of a NMR methodology, the final goal of which is to compare in detail protein structures in solution This technique will enable us to test the hypothesis that all of these calcium binding proteins have homologous structures. The technique is based upon the substitution of paramagnetic lanthanide ions for the calcium ions and the subsequent analysis in structural terms of the shifts and broadenings induced in the NMR spectrum (^{1}H NMR in this specific example). Our approach is to study carp parvalbumin initially and to use the known X-ray structure of this protein to determine the unknown parameters of the NMR experiment which are required before the shifts and broadenings can be interpreted in terms of the structure of the protein. With these parameters and the knowledge of the amino acid substitutions for different proteins, we will then be able to compare the calculated and observed NMR spectra of a new protein as a probe of its structure.

In this paper we focus on the analysis of the line broadening of the lanthanide-shifted ^{1}H NMR resonances as a method for the determination of metal–proton distances in the EF site

† From the Department of Biochemistry and MRC Group on Protein Structure and Function, University of Alberta, Edmonton, Alberta, T6G 2H7 Canada. *Received February 8, 1980.* This work was supported by the Medical Research Council of Canada Group on Protein Structure and Function and the University of Alberta in the form of a Dissertation Fellowship to L.L.

0006-2960/80/0419-3208$01.00/0

of carp parvalbumin. Experiments such as the frequency dependence of the line broadening coupled with an analysis based upon the theories of Vega & Fiat (1976) and Guêron (1975) indicate that a major contribution to the line widths comes from the novel susceptibility relaxation mechanism and that the distances can be directly calculated from this contribution. We have chosen Yb^{3+} for our distance measurements, primarily because the contact interaction is the smallest for Yb^{3+} relative to the other lanthanides (Reuben, 1973). In addition, the ratio of the susceptibility line broadening to the pseudocontact shift is relatively small; this results in comparatively high-resolution spectra for the shifted peaks (Lee & Sykes, 1980a).

Theory

When a paramagnetic trivalent lanthanide (excluding the isotropic Gd^{3+}) is added to a protein metal ion binding site, it will cause shifting and broadening of the NMR resonances of nearby nuclei. If the rates of dissociation of the lanthanide ion from the protein are in the NMR slow exchange limit on the chemical shift time scale, the resultant shifted and broadened resonances will be observed separate from the resonances of the diamagnetic protein. The shifts observed have been analyzed in detail elsewhere (Lee & Sykes, 1980a,b); in this section the focus will be on the line broadening of the shifted resonances.

A given nucleus I in the protein and near the lanthanide ion (Yb^{3+} in this case) will experience relaxation from two sources: other nearby nuclei and the paramagnetic metal. The relaxation caused by the other nuclei will be in form of dipole–dipole (DD) interactions. The results for the spin–lattice relaxation rate ($1/T_{1DD}$) and the spin–spin relaxation rate ($1/T_{2DD}$) are given in eq 1 and 2 for the case of like nuclei with a nuclear spin quantum number $I = 1/2$ (i.e., ^1H's) (Abragam, 1961):

$$\frac{1}{T_{1DD}} = \frac{3\gamma_I^4\hbar^2}{10}\sum\left(\frac{1}{d^6}\right)\left[\frac{\tau_R}{1+(\omega_I\tau_R)^2} + \frac{4\tau_R}{1+4\omega_I^2\tau_R^2}\right] \quad (1)$$

$$\frac{1}{T_{2DD}} = \frac{3\gamma_I^4\hbar^2}{20}\sum\left(\frac{1}{d^6}\right)\left(3\tau_R + \frac{5\tau_R}{1+\omega_I^2\tau_R^2} + \frac{2\tau_R}{1+4\omega_I^2\tau_R^2}\right) \quad (2)$$

γ_I is the gyromagnetic ratio of the nucleus I, τ_R is the rotational correlation time of the metal–protein complex, ω_I is resonance frequency of nucleus I, and $\sum(1/d^6)$ represents the weighted summed distance between the proton under observation and nearby protons.

The relaxation caused by the unpaired 4f electrons of the metal will involve three contributions in general: scalar or contact interactions, dipolar interactions, and the novel "susceptibility" mechanism. In our discussion we will neglect the contact interactions which result from electron delocalization (Bloembergen, 1957) at the nucleus of interest because (1) the 4f electrons are not highly delocalized (when compared to the transition metal 3d electrons, for example), (2) all the protons of interest are many bonds removed from the metal, and (3) within the lanthanide series the contact interactions are the smallest for ytterbium (Reuben, 1973).

The dipolar interaction of the observed nuclei with the 4f electrons, presented in eq 3 and 4 (Solomon, 1955), is of the same form as that presented elsewhere for the transition metals or spin-labels except for the replacement of the electronic g factor by the Landé g_L factor and the spin angular momentum S by the total angular momentum J.[1]

$$\frac{1}{T_{1S}} = \frac{2}{15}\frac{\gamma_I^2 g_L^2\beta^2 J(J+1)}{r^6}\left(\frac{3\tau_S}{1+\omega_I^2\tau_S^2} + \frac{7\tau_S}{1+\omega_S^2\tau_S^2}\right) \quad (3)$$

$$\frac{1}{T_{2S}} = \frac{1}{15}\frac{\gamma_I^2 g_L^2\beta^2 J(J+1)}{r^6}\left[4\tau_S + \frac{3\tau_S}{1+(\omega_I\tau_S)^2} + \frac{13\tau_S}{1+(\omega_S\tau_S)^2}\right] \quad (4)$$

τ_S is the electron correlation time, ω_S is the electron spin frequency ($= 657\omega_I$), β is the Bohr magneton for the electron, and r is the metal to proton distance. This expression assumes that the longitudinal and transverse relaxation times of the electron are both equal to τ_S and the τ_S is much less than τ_R (for Yb^{3+}, τ_S will be of the order of 10^{-13}–10^{-12} s).

The novel element not considered in previous discussions of nuclear spin relaxation caused by paramagnetic metals such as Mn^{2+} and Gd^{3+} is that the time average of the dipolar interaction (on a time scale $\tau_S < t < \tau_R$) is not zero but results in an electronic spin moment μ at the metal related to the magnetic susceptibility by $\mu = \mathbf{X}\cdot\mathbf{H}$. The dipolar interaction of the nuclei with this moment is modulated by the rotational tumbling of the protein–metal ion complex, which results in the "susceptibility" (Vega & Fiat, 1976) or "Curie spin" (Gueron, 1975) contribution to the relaxation. Since the leading term in the susceptibility is isotropic (Bleaney, 1972), this contribution presented in eq 5 and 6 is not dependent upon the angular orientation of the nucleus relative to the metal (Vega & Fiat, 1976):

$$\frac{1}{T_{1\chi}} = \frac{6}{5}\frac{\omega_I^2 g_L^4\beta^4 J^2(J+1)^2}{r^6(3kT)^2}\left(\frac{\tau_R}{1+\omega_I^2\tau_R^2}\right) \quad (5)$$

$$\frac{1}{T_{2\chi}} = \frac{1}{5}\frac{\omega_I^2 g_L^4\beta^4 J^2(J+1)^2}{r^6(3kT)^2}\left[4\tau_R + \frac{3\tau_R}{1+(\omega_I^2\tau_R^2)}\right] \quad (6)$$

k is the Boltzmann constant and T is the temperature.

In fact the average of this interaction is not zero but results in the lanthanide pseudocontact shift which depends upon the angular orientation of the nucleus relative to the lanthanide. A correction term in the form of the multiplicative factor

$$1 - \frac{r^3\delta}{\bar{\chi}} \quad (7)$$

can then be applied to eq 5 and 6 (Vega and Fiat, 1976) if warranted, where δ is the observed lanthanide-induced shift of the observed resonance and $\bar{\chi}$ is the trace of the susceptibility tensor.

Experimental Procedures

NMR Procedures. ^1H NMR spectra were obtained on Bruker WP-200, HXS-270, and WH-400 NMR spectrometers operating in the Fourier transform mode with quadrature detection. Typical instrumental settings for the 270-MHz spectra, from which most of the data were obtained, were acquisition time 0.2 s, sweep width ±10 kHz,, spectrum size

[1] For the lanthanide 4f electrons, the crystal field effects are relatively small so that the L and S angular momenta are coupled to form total angular momentum J states. The appropriate Hamiltonian is $H = g_L\beta(\mathbf{H}\cdot\mathbf{J})$ + correction terms (Bleaney, 1972).

8192 data points, and line broadening 5 Hz. No HDO homonuclear decoupling was employed. The sample temperature was 303 K. The chemical shifts were measured relative to the principal resonance of sodium 2,2-dimethyl-2-silapentane-5-sulfonate (DSS)[2] as an internal standard. The standard filters on the HXS-270 spectrometer were replaced with Bessel filters (Ithaco, Model 4302). Spectra were taken with a filter width set equal to twice the spectral width which results in minimum base line distortion. The spin–lattice relaxation times (T_1) were measured with the standard $T-\pi-\tau-\pi/2-$ acquisition pulse sequence with $T > 5T_1$ and a variable time delay, τ.

Spin–spin relaxation rates were measured from the half-height line widths ($\Delta\nu$) of the observed shifted resonances: $1/T_2 = \pi\Delta\nu$. These were corrected by subtracting the line broadening used during Fourier transformation. No correction was attempted for the possible multiplet structure of some of the resonances from unresolved spin–spin coupling. The observed line broadening is much greater than the possible coupling constants so that all nonoverlapping shifted resonances appeared completely Lorentzian and any corrections would be small.

Spin–lattice relaxation rates ($1/T_1$) were determined by using a nonlinear least-squares fit of the data to the equation

$$M_Z(t) = M_0[1 - (1 - \cos\alpha)e^{-t/T_1}]$$

with the equilibrium magnetization M_0, the flip angle α, and the spin–lattice relaxation rate T_1 as parameters. The value of α was uniform across the spectrum.

Sample Preparation. Stock ytterbium solutions were prepared from dried Johnson-Matthey ultrapure oxides as discussed earlier (Birnbaum & Sykes, 1978).

The concentration of Yb^{3+} was determined by titration with EDTA in pH 6 Mes [2-(*N*-morpholino)ethanesulfonic acid] buffer using xylenol orange as an indicator.

Carp parvalbumin (p*I* = 4.25) was isolated by the method of Pechère et al. (1971). The purity and identity of this isotype were confirmed by slab gel electrophoresis, ultraviolet absorption spectrometry, and amino acid analysis. The protein used was Ca^{2+} saturated as evidenced by comparison with the ^1H NMR spectra of apo and Ca^{2+}-saturated parvalbumin and by crystallization of the protein since the apo form does not crystallize (Kretsinger & Nockolds, 1973).

The NMR samples were prepared by dissolving the lyophilized protein in D_2O buffer, 15 mM Pipes, 0.15 M KCl, 10 mM DTT, and 0.5 mM DSS, pH 6.6. pH measurements were made with an Ingold microelectrode (Model 6030-04) attached to a Beckman Expandomatic SS-2 or a Radiometer 26 pH meter. The pH values quoted are those observed and are not corrected for the deuterium isotope effect on the glass electrode. Protein concentrations were determined by amino acid analysis after 24 h of acid hydrolysis at 110 °C. The Yb^{3+} titrations were performed by the addition of 10-μL aliquots of Yb^{3+}, prepared at the same pH as the protein sample, pH 6.6. The addition of Yb^{3+} did not affect the final pH of the resulting protein solution.

Results

The substitution of Yb^{3+} for one or both of the calcium ions of parvalbumin causes a series of shifted resonances to appear in the ^1H NMR spectrum far outside of the envelope of the spectrum of the calcium form of the protein (Lee & Sykes, 1980a,b). When Yb^{3+} was added to the Ca^{2+}-saturated parvalbumin in these experiments, the sequential appearance and disappearance of several sets of shifted peaks were observed. Up to a ratio of total Yb^{3+} to total parvalbumin (Yb_0/P_0) of $\sim$1/1, one set of peaks appeared. At higher Yb_0/P_0 ratios in the range of $\sim$1:1 to $\sim$2:1, some of the first set of peaks corresponding to nuclei near the site of the first calcium replaced but removed from the second site were not affected, whereas some of the first set of peaks corresponding to nuclei near both metal binding sites disappeared (shifted elsewhere) and were replaced by a new set of peaks. These results indicate the Yb^{3+} sequentially replaces the two Ca^{2+} ions of parvalbumin and that the rates of dissociation of the lanthanide from the protein are slow enough that the NMR spectra are in the slow exchange limit. Several experiments indicate that the EF calcium is replaced first by lanthanides (Lee & Sykes, 1980a,b). These include X-ray studies of the isomorphous replacement of the EF Ca^{2+} of parvalbumin by Tb^{3+} at low Tb_0/P_0 ratios (Sowadski et al., 1978), Tb^{3+} fluorescence experiments (Donato & Martin, 1974), and laser-induced luminescence experiments with Eu^{3+} or Tb^{3+} (Horrocks & Sudnick, 1979). The shifted peaks are shown in Figure 1B for Yb^{3+} at a Yb_0/P_0 ratio of 0.80. Since these spectra are in the NMR slow exchange limit, the shifted resonances in Figure 1B represent the spectrum of the parvalbumin–one Ca^2 (CD)–one Yb^{3+} (EF) complex.

The shifted peaks are shown in expansion in Figure 2 with the nomenclature that is used in the rest of the manuscript. Overlapping resonances were resolved by following the positions of the shifted peaks (which all move differently) as a function of temperature (Lee & Sykes, 1980b). Only the resonances which appear as single resolved peaks at 303 K are discussed in this manuscript.

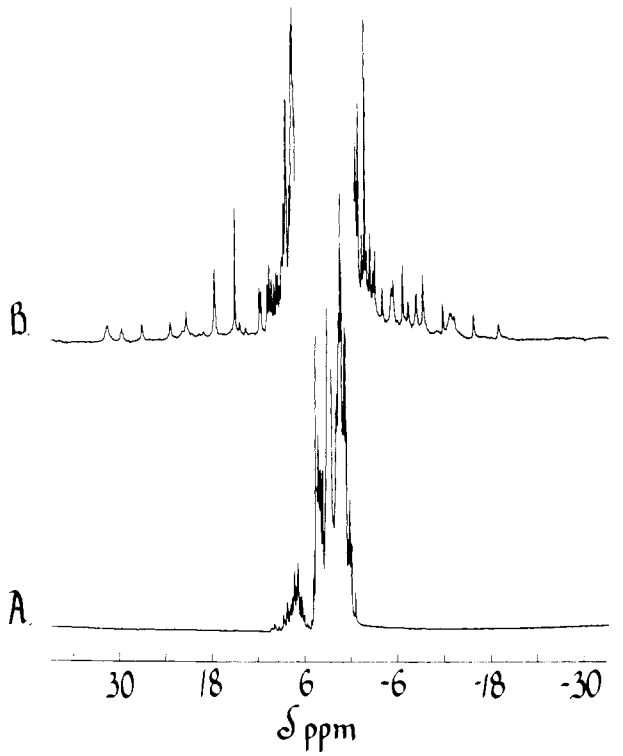

FIGURE 1: 270-MHz ^1H NMR spectrum of (A) 0.68 mM calcium saturated carp parvalbumin in 15 mM Pipes, 0.15 M KCl 0.5 mM DSS, 10 mM DTT, and D_2O, pH 6.65, temperature = 303 K, and (B) 0.64 mM carp parvalbumin in 15 mM Pipes, 0.15 M KCl, 0.5 mM DSS, 10 mM DTT, and D_2O, pH 6.6, temperature = 303 K, at a total Yb^{3+}/total protein ratio (Yb_0/P_0) of 0.80. The vertical scale for (B) is 8× that for (A).

[2] Abbreviations used: EDTA, ethylenediaminetetraacetic acid; DSS, sodium 2,2-dimethyl-2-silapentane-5-sulfonate; DTT, dithiothreitol; Mes, 2-(*N*-morpholino)ethanesulfonic acid; Pipes, piperazine-*N*,*N*′-bis(2-ethanesulfonic acid).

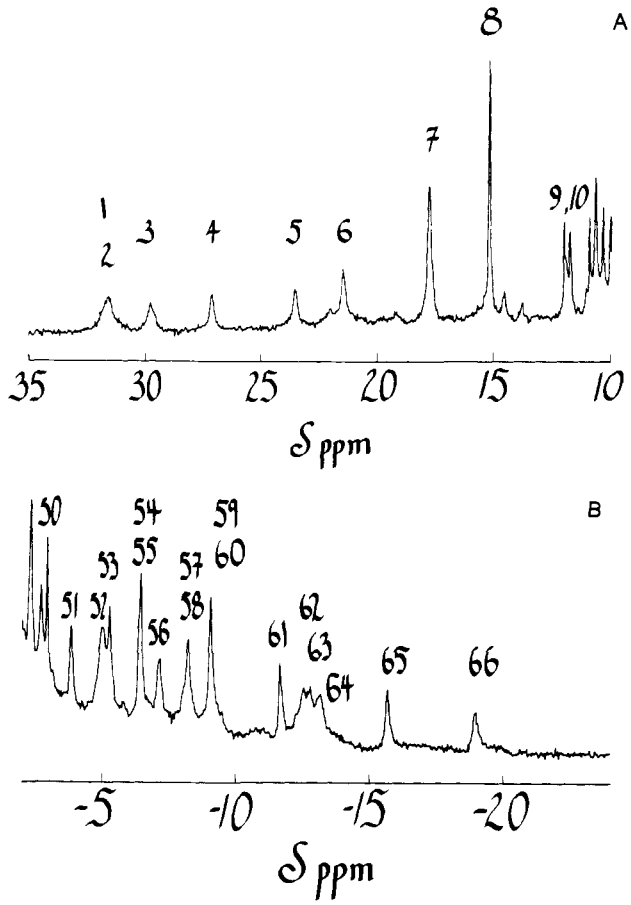

FIGURE 2: 270-MHz ^{1}H NMR spectrum of ytterbium-substituted parvalbumin. Conditions are the same as those indicated in the legend for Figure 1B. Indicated are peak nomenclature and chemical shifts, measured relative to the principal resonance of DSS. (A) Downfield regions; (B) Upfield region.

Table I: Spin–Spin Relaxation Rates of the Ytterbium-Shifted Parvalbumin Resonances as a Function of ^{1}H NMR Resonance Frequency

reso-nance[a]	obsd shift (ppm)[a]	$1/T_2$ (s^{-1}) 200 MHz	270 MHz	400 MHz
3	29.80	278	303	500
4	27.16	179	213	400
5	23.57	217	263	385
6	21.50	185	256	323
7	17.79	161	189	323
8	15.17	85	94	125
10	11.75	101	120	125
51	−3.84	114	103	152
56	−7.11	161	179	323
61	−11.63	127	137	200
65	−15.65	175	179	278
66	−18.90	170	213	455

[a] Nomenclature and chemical shifts correspond to data presented in Figure 2.

The corrected line widths of the observed shifted resonance which are clearly resolved single peaks are presented in Table I at three ^{1}H NMR frequencies: 200, 270, and 400 MHz. A typical plot of the spin–spin relaxation rates ($1/T_2$) of the peaks numbered 5 and 6 at 23.57 and 15.17 ppm, respectively, as a function of ω_I^2, the square of the resonance frequency in units of radians per second, is presented in Figure 3. The subsequent separation of the line widths into two contributions, one field independent ($1/T_{2DD}$) and one field dependent ($1/T_{2\chi}$, evaluated at 270 MHz), is tabulated in Table II. Also

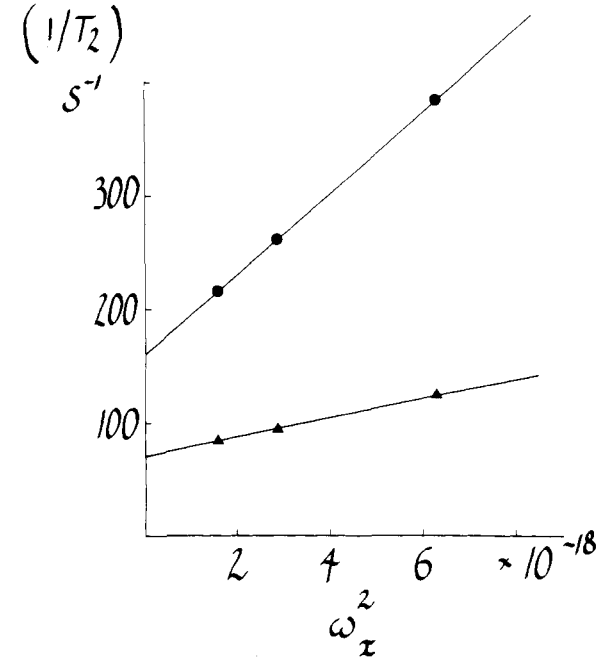

FIGURE 3: Plot of the observed spin–spin relaxation rates ($1/T_2$) vs. the square of the resonance frequency (ω_I^2) in units of radians per second. The (●) indicates data observed for resonance 5 with δ = 23.57 ppm; the (▲) indicates data observed for resonance 8 with δ = 15.17 ppm. Line widths were measured at 200, 270, and 400 MHz.

Table II: Relative Contributions of Various Mechanisms to Spin–Spin Relaxation of Shifted ^{1}H NMR Resonances in Ytterbium-Substituted Parvalbumin Determined from the ^{1}H NMR Resonance Frequency Dependence of the Observed Line Widths

reso-nance[a]	$1/T_{2DD}$ (s^{-1})[b]	$1/T_{2\chi}$ (s^{-1})[c]	r (A)[d]
3	184	325	$5.8^{+0.1}_{-0.1}$
4	91	230	$5.9^{+0.1}_{-0.1}$
5	161	263	$6.2^{+0.2}_{-0.2}$
6	157	235	$6.5^{+0.3}_{-0.2}$
7	98	199	$6.2^{+0.2}_{-0.2}$
8	71	95	$7.9^{+1.8}_{-0.7}$
10	100	112	$8.8^{+1.4}_{-1.2}$
51	90	116	$7.7^{+1.5}_{-0.6}$
56	93	195	$6.2^{+0.2}_{-0.2}$
61	97	143	$7.0^{+0.6}_{-0.4}$
65	127	194	$6.6^{+0.3}_{-0.2}$
66	56	235	$5.6^{+0.1}_{-0.1}$

[a] Nomenclature corresponds to data presented in Figure 2. [b] $1/T_{2DD}$ was determined by a linear least-squares fit to the data. [c] $1/T_{2\chi}$ was determined by a linear least-squares fit to the data and corresponds to the calculated value at 270 MHz. [d] r, the metal–nucleus distance, was calculated by using data in column 3 and eq 14.

tabulated in Table II are the calculated metal to proton distances for each peak with estimated error limits (see Discussion). The measured T_1 values at 270 MHz for each peak are listed in Table III, along with an estimated T_{1S} corrected

Table III: Measured Spin-Lattice Relaxation Times for Ytterbium-Shifted ^{1}H NMR Resonances of Parvalbumin

resonance[a]	T_1 (s)[b]	T_{1S} (s)[c]	$1/T_{2X}$ (s^{-1})	T_{1S}/T_{2X}
3	0.032	0.033-0.035	325	10.7-11.4
4	0.054	0.057-0.063	230	13.1-14.5
5	0.046	0.048-0.052	263	12.6-13.7
6	0.043	0.045-0.048	235	10.6-11.3
7	0.046	0.048-0.052	199	9.6-10.3
8	0.145	0.167-0.233	93	15.5-21.7
10	>0.3[d]		112	
51	0.240	0.305-0.637	116	35.5-73.9
56	0.138	0.157-0.215	195	30.6-41.9
61	0.252	0.326-0.730	143	46.6-104.4
65	0.164	0.192-0.286	194	37.2-55.5
66	0.098	0.108-0.132	235	25.4-31.0

[a] Nomenclature corresponds to data presented in Figure 2. [b] These observed T_1 values were measured at 270 MHz by inversion recovery pulse sequences. [c] T_{1S} indicates spin-lattice relaxation times which are corrected for proton-proton dipole-dipole relaxation contributions (see Discussion). These contributions were observed to be in the range of 0.9 s^{-1} for aromatic protons and 2.6 s^{-1} for methylene protons at 270 MHz. [d] Delay time used in T_1 measurement was not sufficient to accurately determine long T_1.

for the diamagnetic contribution to the spin–lattice relaxation (see Discussion) and the ratio of the estimated T_{1S} to the measured T_{2X}.

Discussion

We have proposed a strategy for the complete analysis of the lanthanide-induced ^{1}H NMR chemical shifts of the ytterbium–parvalbumin complex in order to determine the three-dimensional structure of the EF binding domain of parvalbumin in solution. As a part of the overall approach, we discuss in this paper the determination of metal–nucleus distances from an analysis of the line widths and spin–lattice relaxation rates of the shifted resonances. Lanthanide-induced ^{1}H NMR shifts have been used previously to probe the structure of lysozyme and the bovine pancreatic trypsin inhibitor (Campbell et al., 1975; Agresti et al., 1977; Marinetti et al., 1975, 1976, 1977). Neither of these proteins have high-affinity specific metal binding sites. In both of these examples the ^{1}H NMR spectra are in the fast exchange limit. This has the advantage that assigned resonances may be followed as a function of metal concentration. It has, however, the disadvantage that shifts and line widths or relaxation rates characterizing the protein–metal ion complex can only be obtained by a fitting procedure. This involves data taken at high concentrations of metal ion where nonspecific binding can influence the results. In our case, the protein has high-affinity specific metal binding sites, which result in spectra in the NMR slow exchange limit (Figure 1B). The advantage here is that the chemical shifts and relaxation rates of the parvalbumin–paramagnetic ion complex may be accurately and directly determined. The main disadvantage is the assignment of the observed resonance.

The substitution of calcium in parvalbumin by ytterbium at a Yb_0/P_0 ratio of 0.80 results in a series of shifted resonances in the NMR slow exchange limit as seen in Figure 1B. As reviewed under Results (Lee & Sykes, 1980a,b), the Ca^{2+} ions of parvalbumin are sequentially replaced by Yb^{3+}; only one Ca^{2+} is replaced by Yb^{3+} at a Yb_0/P_0 ratio of 0.80, and we conclude that the substitution occurs initially in the EF site by analogy to X-ray crystallographic data and optical studies (Horrocks & Sudnick, 1979; Sowadski et al., 1978; Donato & Martin, 1974). Before analyzing the nuclear spin relaxation of the shifted resonances, it is important to determine whether or not there is significant exchange contribution to the line widths. The exchange braodening is equal to k_{off}/π in the slow exchange limit, where k_{off} is the dissociation rate constant for Yb^{3+} from the EF binding site of parvalbumin. Since this exchange broadening is the same for all resonances, whereas a wide variation in line widths is observed, the exchange broadening cannot dominate the observed line width except possibly for the narrowest resonances. From the fact that the Yb^{3+} replaces the Ca^{2+} from the first site when only stoichiometric amounts of Yb^{3+} are added (Lee & Sykes, 1980a,b), we can conclude that the binding of Yb^{3+} to the EF site is stronger than the binding of Ca^{2+} to that site. A dissociation rate constant of 0.5 s^{-1} for Ca^{2+} from parvalbumin has been measured by fluoresence stopped-flow methods (Potter et al., 1978). Since the association rate is near the diffusion-controlled limit (Potter et al., 1978), the tighter binding of Yb^{3+} implies a smaller dissociation rate constant. The exchange line broadening can therefore be estimated at <0.1 s^{-1}, which is insignificant for all resonances.

As discussed under Theory, the three possible sources of nuclear spin relaxation of the shifted resonances are dipolar interactions with other nuclei, with the unpaired electrons on the metal, and with the Curie spin moment on the metal (the susceptibility relaxation). The relative contributions of the electronic dipolar relaxation and susceptibility relaxation to the nuclear spin–spin relaxation rates are given by (Vega & Fiat, 1976)

$$\frac{1/T_{2X}}{1/T_{2S}} = \frac{4}{7}\Delta\frac{\tau_R}{\tau_S} \tag{8}$$

in the limit $\omega_0\tau_R > 1$, where Δ is defined as

$$\Delta = \frac{21}{20}\frac{g_L^2\beta^2J(J+1)H_0^2}{(3kT)^2} \tag{9}$$

Similarly, the relative contribution of the electronic dipolar and susceptibility mechanism to the spin–lattice relaxation rates is given by

$$\frac{1/T_{1X}}{1/T_{1S}} = \frac{6}{7}\frac{1}{\omega_I^2\tau_R^2}\Delta\frac{\tau_R}{\tau_S} \tag{10}$$

For evaluation of eq 8–10, the following constants are substituted: $g_L = 8/7$ and $J = 7/2$ for Yb^{3+}, $H_0 = 63\,000$ G, $\omega_I = (270)(2\pi) \times 10^6$ rad s^{-1}, and $T = 300$ K. A value for the rotational correlation time τ_R of 12×10^{-9} s has been measured for parvalbumin by ^{13}C NMR and light scattering (Nelson et al., 1976; Bauer et al., 1975). The only number which is not known exactly is the electron spin relaxation time τ_S, although τ_S is known to be of the order of 10^{-13}–10^{-12} s. Choosing τ_S to be 2×10^{-13} s, which we will show is consistent with the value calculated from the experimental results (see below), eq 8 and 10 become

$$\frac{1/T_{2X}}{1/T_{2S}} \simeq 16 \tag{11}$$

$$\frac{1/T_{2X}}{1/T_{1S}} \simeq 0.06 \tag{12}$$

indicating that the electronic contribution for Yb^{3+} to the spin–spin relaxation is dominated by the susceptibility contribution whereas the contribution to the spin–lattice relaxation is dominated by the electronic dipolar relaxation.

The line width is thus made up from two contributions, electronic susceptibility and nuclear dipole interactions. In

the limit $\omega_I\tau_R > 1$, the first contribution is proportional to ω_I^2 and the second contribution is field independent. These two contributions can thereby be separated by the dependence of the line width on the field. We have determined the line widths of the shifted resonances at 200, 270, and 400 MHz (see Table I and Figure 3), and a ω_I^2 field dependence is observed which allows us to obtain measured values of $1/T_{2\chi}$ and $1/T_{2DD}$.

The contributions to the spin–lattice relaxation cannot be as easily separated, since the electronic dipolar contributions are not field dependent ($\omega_I\tau_S$ and $\omega_S\tau_S \ll 1$) unless τ_S is field dependent, and the nulear dipolar contributions can be influenced by other considerations such as spin diffusion. The spin–lattice relaxation rates ($1/T_1$) have been measured for the calcium-saturated protein at 270 MHz and range from 0.9 to 2.6 s^{-1} for various peaks across the spectrum. We can then estimate the range of possible values of T_{1S} at 270 MHz for each shifted peak from the measured relaxation rate by subtracting the minimum and maximum values of $1/T_{1DD}$ observed for the diamagnetic protein. These values are listed in Table III.

We are thus able to obtain a possible range of values of $1/T_{1S}$ and a measured value of $1/T_{2\chi}$ and $1/T_{2DD}$ for each peak. At 270 MHz, the expressions for T_{1S} and $T_{2\chi}$ reduce to

$$\frac{1}{T_{1S}} = \frac{1.69 \times 10^{-30}}{r^6}\tau_S \qquad (13)$$

$$\frac{1}{T_{2\chi}} = \frac{5.60 \times 10^{-42}}{r^6}\left(1 - \frac{r^3\delta}{\bar{\chi}}\right) \qquad (14)$$

The correction term from eq 7 shown in eq 14 is expected to be small. In addition, it is approximately constant (except for a change in sign in δ) because $\bar{\chi}$ is dominated by the first term in an expansion in $1/T$ which is isotropic and δ is proportional (omitting angular factors for the moment) to $1/r^3$ (Bleaney, 1972). This predicts that the ratio $T_{1S}/T_{2\chi}$ should be approximately constant although possibly different for both the low-field shifted peaks and the high-field shifted peaks, as is observed (see Table III). The value of the correction factor $r^3\delta/\bar{\chi}$ may be estimated from an individual peak such as no. 4, for which we have a shift from its diamagnetic position of 20.10 ppm (Lee & Sykes, 1980b), r = 5.9 Å (calculated neglecting the correction factor), and $\bar{\chi} \simeq g_L^2\beta^2J(J+1)/(3kT) = 1.43 \times 10^{-26}$ cm^3, yielding $r^3\delta/\bar{\chi} \simeq 0.28$. The individual distances presented in Table II do not take this correction factor into account, since it could vary slightly from peak to peak because of the dependence of δ on the angular orientation of the particular nucleus relative to the metal. The error this makes in the distance is $\sim\pm4\%$, which is less than the error from other sources. The value of τ_S calculated from the $T_{1S}/T_{2\chi}$ ratio for peak 4 neglecting the correction factor is 2.4×10^{-13} s.

The distances calculated from the measured value of $1/T_{2\chi}$ at 270 MHz and eq 14 neglecting the correction factor as discussed above are presented in Table II. As one can see, the shifted peaks represent nuclei fairly closely surrounding the metal ion. For comparison, the two protons bonded to the β carbon of Asp-90 directly chelating the metal are 5.6 and 4.7 Å removed. The errors in the calculated distances were estimated by considering the probable measurement errors at 270 MHz in comparison with the experimentally deduced value of $1/T_{2\chi}$ at 270 MHz. The error in the calculated distances rapidly gets larger as the distance gets longer, as also observed elsewhere (Rowan et al., 1974). Note also that the upper and lower error limits in the distance are not equal because of the inverse sixth power relationship between errors in the observed line widths and errors in the calculated distances. The magnitude of the susceptibility contribution to the line broadening could be increased by the choice of a different lanthanide (Lee & Sykes, 1980a), and this would decrease the errors in the measured distances. We have, however, chosen ytterbium because the contact interactions are the smallest with respect to the other lanthanides and the ratio of the pseudocontact shift to the contact shift is the largest (Reuben, 1973). Also, the ratio of the pseudocontact shift to the susceptibility line broadening is relatively large (Lee & Sykes, 1980a), resulting in a relatively high-resolution spectrum for the shifted resonances.

The experimentally determined values for the contributions to the line widths of the shifted resonances from other nuclei ($\Delta\nu_{DD} = 1/\pi T_{2DD}$) range from 18 to 59 Hz (see Table III). This range is appropriate for a protein of the size of parvalbumin. For comparison, the calculated line width of an isolated rigid CH_2 pair (which would represent the shortest possible proton–proton distance), such as the Asp β protons, on a protein with a rotational correlation time of 12×10^{-9} s is 28 Hz, below the upper limit of the experimental values.

In conclusion, we have shown how the nuclear spin relaxation of nuclei near a bound lanthanide metal ion in a protein can be analyzed to yield the distance between the nuclei and the metal ion. We have applied this approach to the nuclei directly surrounding the EF calcium binding domain of carp parvalbumin. The distances calculated for the shifted resonances are part of an attempt to determine the structure of the EF calcium binding domain of parvalbumin in solution, which also includes the elucidation of the angular orientation of the shifted nuclei relative to the metal from an analysis of the observed shifts.

Acknowledgments

We acknowledge many helpful discussions with Dr. Timothy D. Marinetti and with Dr. Edward R. Birnbaum, whose initial observation of the lanthanide-shifted resonances of the troponin C–CB-9-Pr^{3+} complex (Lee et al., 1979) lead to much of this present work. The assistance of Drs. Louis Delbaere and Brian F. P. Edwards in calculating the X-ray based proton coordinates, Dr. William E. Hull, Dr. Tom Nakashima, and Glen Bigam for running the 400- and 200-MHz NMR spectra, and Mike Natriss for running amino acid analyses is also gratefully acknowledged.

References

Abragam, A. (1961) *The Principles of Nuclear Magnetism*, pp 264–353, Oxford University Press, London and New York.

Agresti, D. G., Lenkinski, R. E., & Glickson, J. D. (1977) *Biochem. Biophys. Res. Commun. 76*, 711–719.

Bauer, D. R., Opella, S. J., Nelson, D. J., & Pecora, R. (1975) *J. Am. Chem. Soc. 97*, 2580–2582.

Birnbaum, E. R., & Sykes, B. D. (1978) *Biochemistry 17*, 4965–4971.

Bleaney, B. (1972) *J. Magn. Reson. 8*, 91–100.

Bloembergen, N. (1957) *J. Chem. Phys. 27*, 572–573, 595–596.

Campbell, I. D., Dobson, C. M., & Williams, R. J. P. (1975) *Proc. R. Soc. London, Ser. A 345*, 41–59.

Cheung, W. Y. (1980) *Science 207*, 19–27.

Collins, J. H. (1974) *Biochem. Biophys. Res. Commun. 58*, 301–308.

Collins, J. H. (1976) *Nature (London) 259*, 699–700.

Dabrowska, R., Sherry, J. M. F., Aromatorio, D. K., & Hartshorne, D. J. (1978) *Biochemistry 17*, 253–258.
Dedman, J. R., Jackson, R. L., Schreiber, W. E., & Means, A. R. (1978) *J. Biol. Chem. 253*, 343–346.
Donato, H., Jr., & Martin, R. B. (1974) *Biochemistry 13*, 4575–4579.
Fullmer, C. S., & Wasserman, R. H. (1977) *Calcium Binding Proteins and Calcium Function* (Wasserman, R. H., Corradino, R. A., Carafoli, E., Kretsinger, R. H., MacLennan, D. H., Siegel, F. L., Eds.) pp 302–303, Elsevier, New York.
Guêron, M. (1975) *J. Magn. Reson. 19*, 58–66.
Hofmann, T., Kawakami, M., Hitchman, A. J. W., Harrison, J. E., & Dorrington, K. J. (1979) *Can. J. Biochem. 57*, 737–748.
Horrocks, W. DeW., Jr., Sudnick, D. R. (1979) *J. Am. Chem. Soc. 101*, 334–340.
Kretsinger, R. H. (1976) *Annu. Rev. Biochem. 45*, 239–266.
Kretsinger, R. H., & Nockolds, C. E. (1973) *J. Biol. Chem. 248*, 3313–3326.
Lee, L., & Sykes, B. D. (1980a) *Methods for Determining Metal Ion Environments in Proteins: Structure and Function of Metalloproteins* (Darnall, D. W., & Wilkins, R. G., Eds.) pp 183–210, Elsevier North-Holland, New York.
Lee, L., & Sykes, B. D. (1980b) *Biophys. J.* (in press).
Lee, L., Sykes, B. D., & Birnbaum, E. R. (1979) *FEBS Lett. 98*, 169–172.
Lin, Y. M., Liu, Y. P., & Cheung, W. Y. (1974) *J. Biol. Chem. 249*, 4943–4954.
Marinetti, T. D., Snyder, G. H., & Sykes, B. D. (1975) *J. Am. Chem. Soc. 97*, 6562–6570.
Marinetti, T. D., Snyder, G. H., & Sykes, B. D. (1976) *Biochemistry 15*, 4600–4608.
Marinetti, T. D., Snyder, G. H., & Sykes, B. D. (1977) *Biochemistry 16*, 647–653.
Nelson, D. J., Opella, S. J., & Jardetzky, O. (1976) *Biochemistry 15*, 5552–5560.
Pechère, J.-F., Demaille, J., & Capony, J.-P. (1971) *Biochim. Biophys. Acta 236*, 391–408.
Potter, J. D., Johnson, J. D., Dedman, J. R., Schreiber, W. E., Mandel, F., Jackson, R. L., & Means, A. R. (1977) *Calcium Binding Proteins and Calcium Function* (Wasserman, R. H., Corradino, R. A., Carafoli, E., Kretsinger, R. H., MacLennan, D. H., & Siegel, F. L., Eds.) pp 239–249, Elsevier, New York.
Potter, J. D., Johnson, J. D., & Mandel, F. (1978) *Fed. Proc., Fed. Am. Soc. Exp. Biol. 37*, 1608.
Rasmussen, H., Goodman, D. B. P., & Tenehouse, A. (1972) *CRC Crit. Rev. Biochem. 1*, 95–148.
Reuben, J. (1973) *J. Magn. Reson. 11*, 103–104.
Rowan, R., III, McCammon, J. A., & Sykes, B. D. (1974) *J. Am. Chem. Soc. 96*, 4773–4780.
Solomon, I. (1955) *Phys. Rev. 99*, 559–565.
Sowadski, J., Cornick, G., & Kretsinger, R. H. (1978) *J. Mol. Biol. 124*, 123–132.
Stevens, F. C., Walsh, M., Ho, H. C., Teo, T. S., & Wang, J. H. (1976) *J. Biol. Chem. 251*, 4495–4500.
Vanaman, T. C., Sharief, F., & Watterson, D. M. (1977) *Calcium Binding Proteins and Calcium Function* (Wasserman, R. H., Corradino, R. A., Carafoli, E., Kretsinger, R. H., MacLennan, D. H., & Siegel, F. L., Eds.) pp 107–116, Elsevier, New York.
Vega, A. J., & Fiat, D. (1976) *Mol. Phys. 31*, 347–355.
Weeds, A. G., & McLachlan, A. D. (1974) *Nature (London) 252*, 646–649.
Weeds, A., Wagner, P., Jakes, R., & Kendrick-Jones, J. (1977) *Calcium Binding Proteins and Calcium Function* (Wasserman, R. H., Corradino, R. A., Carafoli, E., Kretsinger, R. H., MacLennan, D. H., Siegel, F. L., Eds.) pp 222–231, Elsevier, New York.
Westcott, K. R., La Porte, D. C., & Storm, D. R. (1979) *Proc. Natl. Acad. Sci. U.S.A. 76*, 204–208.
Yagi, K., Yazawa, M., Kakiuchi, S., Ohshima, M., & Uenishi, K. (1978) *J. Biol. Chem. 253*, 1338–1340.